

circVAPA promotes the proliferation, migration and invasion of oral cancer cells through the miR-132/HOXA7 axis

Journal of International Medical Research
49(6) 1–13

© The Author(s) 2021

Article reuse guidelines:

sagepub.com/journals-permissions

DOI: 10.1177/03000605211013207

journals.sagepub.com/home/imr



Hao Chen¹ , Ye Zhang^{2,3}, Kankui Wu⁴ and Xiaoyong Qiu¹ 

Abstract

Objective: To study the relationship between the circular RNA vesicle-associated membrane protein-associated protein A (circVAPA) and the pathogenesis of oral squamous cell carcinoma.

Methods: The expression of circVAPA was detected by RT-qPCR. *In vitro* loss-of-function experiments were performed in Cal-27 cells. The malignant phenotype of cells was evaluated by cell counting kit-8, clone formation and transwell assays. Luciferase reporter assays were used to assess the circVAPA/miR-132/homeobox A (HOXA) regulatory axis.

Results: circVAPA expression was significantly increased in oral cancer tissues and cells. The overall survival and progression-free survival of patients with oral cancer who exhibited high circVAPA expression were significantly shorter compared with those with low expression. circVAPA expression was closely related to tumor size, TNM stage and distant metastasis. circVAPA knockdown reduced the proliferation, invasion and migration of Cal-27 cells. MiR-132 was identified as a target of circVAPA in Cal-27 cells. Cotransfection with si-circVAPA and miR-132 inhibitor reversed the inhibitory effect of circVAPA knockdown on cell malignant phenotypes. HOXA7 was further identified as a downstream target of miR-132.

Conclusion: circVAPA is highly expressed in oral cancer, and its abnormal expression might affect the proliferation, invasion and migration of oral cancer cells by modulating the miR-132/HOXA7 signaling axis.

¹Department of Stomatology, the Wuhan Sixth Hospital, Wuhan, China

²Department of Stomatology, the First Affiliated Hospital of Jinan University, Jinan, China

³School of Stomatology, Jinan University, Jinan, China

⁴Department of Stomatology, the Second Affiliated Hospital of Guangzhou Medical University, Guangzhou, China

Corresponding author:

Xiaoyong Qiu, Department of Stomatology, the Wuhan Sixth Hospital, No. 168, HongKong Road, Jiang'an District, Wuhan City, Hubei Province 430015, China.
Email: xcvpik125@163.com



Creative Commons Non Commercial CC BY-NC: This article is distributed under the terms of the Creative

Commons Attribution-NonCommercial 4.0 License (<https://creativecommons.org/licenses/by-nc/4.0/>) which permits non-commercial use, reproduction and distribution of the work without further permission provided the original work is attributed as specified on the SAGE and Open Access pages (<https://us.sagepub.com/en-us/nam/open-access-at-sage>).

Keywords

Oral cancer, circular RNA vesicle-associated membrane protein-associated protein A, miR-132, homeobox A7, circular RNA, malignant phenotype

Date received: 14 November 2020; accepted: 31 March 2021

Introduction

Oral cancer is one of the most common malignant tumors in the head and neck, with squamous cell carcinoma in oral and maxillofacial regions accounting for more than 80%.¹ With the increased use of surgery-based comprehensive therapy, the control rate of tumors has been significantly improved. However, the 5-year survival rate of patients with oral cancer remains at approximately 50%,² mainly due to the local proliferation, invasion and distant metastasis of oral cancer.^{3,4} Cancer proliferation, invasion and metastasis are complex biological processes, and the exact underlying molecular mechanisms remain unclear. Therefore, it is necessary to identify the key regulatory molecules that contribute to oral cancer growth and metastasis.

Circular RNA (circ RNA) is a type of closed-loop noncoding RNA widely present in eukaryotes. circ RNAs play an important role in the occurrence and development of tumors, nervous system diseases and cardiovascular diseases.⁵⁻⁷ Studies have shown that circ RNAs are involved in the occurrence and development of solid tumors and hematological malignancies, especially through their biological function as miRNA sponges.^{8,9} Circ RNA regulates several characteristic processes of tumorigenesis, such as escaping growth inhibitors, maintaining proliferation signals, escaping cell death and aging, promoting angiogenesis, activating invasion and enhancing metastasis.^{10,11} In addition, the abnormal

expression, tissue specificity, diversity and stability of loop RNA in tumor cells make it a potential tumor marker. Previous studies have shown that circ RNA is associated with the malignant progression of oral cancer, suggesting that circ RNA has potential as a biomarker for the early diagnosis of patients with oral cancer.¹² The circ RNA vesicle-associated membrane protein-associated protein A (circVAPA) is abnormally expressed in several malignant tumor tissues, and its dysregulated expression is related to the growth and metastasis of colon cancer and other malignant biological behaviors.¹³ However, there are currently no studies on its involvement in oral cancer. Therefore, this article examined the expression of circVAPA in oral cancer and further explored its regulatory role in the growth and metastasis of oral cancer cells. Our study might shed light on the molecular mechanism and provide a novel therapeutic target for oral cancer treatment.

Materials and methods

Patients and tissue samples

This retrospective study was approved by the Ethics Committee of Wuhan Sixth Hospital and conducted in accordance with the Declaration of Helsinki. Patients with pathologically confirmed oral squamous cell carcinoma were enrolled after written informed consent was obtained. Oral cancer and paracancer tissue samples were collected from patients who

underwent surgical resection at Wuhan Sixth Hospital between 2013 and 2018. All patients were restaged according to the 8th edition of the AJCC Staging system.¹⁴ The clinicopathological data (age, sex, tumor size, differentiation, TNM stage, lymph node metastasis and distant metastasis), survival status and recurrence status of all patients were obtained.

Cell culture and reagents

Oral cancer-derived cell lines (Cal-27, FADU, OECM1, SAS and HSC3) and human oral mucous fibroblasts were obtained from the American Type Culture Collection (Chinese Academy of Sciences Cell Bank, Shanghai, China) and cultured in Dulbecco's Modified Eagle's Medium (DMEM) (Gibco; Life Technologies, Carlsbad, CA, USA) supplemented with 10% (v/v) fetal bovine serum (FBS) (Gibco; Life Technologies) at 37°C in a 5% CO₂ incubator. Cells were grown in a monolayer and passaged routinely two to three times a week. Dimethyl sulfoxide and crystal violet were purchased from Sigma (St. Louis, MO, USA).

Plasmid and siRNA transfections

A fragment encoding human circVAPA with a FLAG-tag was generated by PCR amplification. circVAPA was subcloned into the EcoRI and XhoI sites of a lentivirus vector (pLVPT) (Invitrogen, Waltham, MA, USA). Cells were transfected using Lipofectamine 2000 (Invitrogen) following the manufacturer's instructions. The negative control (NC) siRNA and siRNAs against circVAPA were synthesized by Shanghai GenePharma Co., Ltd (Shanghai, China) with the following primers: si-circVAPA#1: 5'-ATGATAAATTGGCCCCTTC-3', si-circVAPA#2: 5'-TAAATTGGCCCCTTCACAG-3' and NC: 5'-TTCTCCGAACGTGTCACGT-3'.

Cell counting kit-8 (CCK-8) assay for cell proliferation

Cells were seeded in 96-well plates containing complete medium at a density of 5×10^3 cells/well and incubated for 24 hours. Five biological replicates were included in each experimental group. After transfection, cells were incubated for 48 hours before the CCK assay. Next, 10 μ L CCK-8 solution was added to each well for 1 hour. The absorbance at 450 nm (A450) was measured with a microplate reader (DR-200Bs, Diatek, West Bengal, India). The proliferation inhibition rate was calculated as follows: proliferation inhibition (%) = $[\text{A450 (negative control group)} - \text{A450 (experimental group)}] / [\text{A450 (negative control group)} - \text{A450 (blank control group)}] \times 100\%$.

Clone formation experiment

Cal-27 cells in the logarithmic growth phase were collected, seeded in a six-well plate at a density of 500 cells/well and cultured in a 37°C, 5% CO₂ incubator for 24 hours. Then, the cells were transfected with siRNA and incubated for 48 hours. After culturing for 15 days, the cells were fixed in methanol and stained with 0.1% crystal violet for 15 to 30 minutes. After washing several times, the plate was placed at room temperature to dry and then photographed. Crystal violet was dissolved in 10% glacial acetic acid, and the absorbance at an optical density of 560 nm was measured using a microplate reader for statistical analysis.

Transwell migration and invasion assay

Transwell polycarbonate membrane cell culture inserts with 8.0- μ m pores (Corning Inc., Corning, NY, USA) were uncoated for migration assays or coated with 50 μ L BD Matrigel Basement Membrane Matrix (BD Biosciences, San Jose, CA, USA) diluted 1:3 in FBS-free DMEM for invasion

assays. Cal-27 cells (2×10^4) were seeded in the top chamber with serum-free medium, allowed to migrate toward serum-containing medium in the lower chamber for 24 hours and then stained with 0.01% crystal violet (AS1086, ASPEN, San Diego, CA, USA) for 10 minutes. The number of cells that invaded through the membrane was counted under a light microscope (five random fields per well) (Leica, Shinjuku, Tokyo, Japan).

Promoter reporters and dual-luciferase assay

Twenty-four hours after being plated in 24-well plates, Cal-27 cells in serum-free medium were transfected with 2 μg of a circVAPA-luciferase reporter construct and 0.02 μg pRL-null expressing *Renilla* luciferase with Lipofectamine 2000 reagent (Life Technologies, Grand Island, NY, USA) for 6 hours in accordance with the manufacturer's instructions. After transfection, cells were cultured in DMEM supplemented with 2% FBS. Thirty-six hours after treatments, cell lysates were prepared and subjected to a dual-luciferase assay in accordance with the manufacturer's instructions (Promega, Madison, WI, USA). Firefly luciferase activity was normalized to *Renilla* luciferase activity.

Quantitative reverse transcription polymerase chain reaction (RT-qPCR)

Cal-27 cells were seeded into 24-well plates (5×10^4 cells per well) for 24 hours. RNA was isolated using Trizol solution (Life Technologies). After the removal of genomic DNA using DNase I (Ambion, Austin, TX, USA), 2.4 μg of total RNA from Cal-27 cells were reverse-transcribed to cDNA using a commercially available kit (Applied Biosystems, Foster City, CA, USA). RT-qPCR was performed with a 7900HT fast real-time PCR system (Applied Biosystems)

using 2 \times SYBR Green master mix (Bio-Rad, Richmond, CA, USA). Forty cycles were performed as follows: 95°C for 30 s and 60°C for 30 s, followed by 1 minute at 72°C for polymerase extension with primers (qPCR miR-132 sense primer 5'-TGCGGGACATTCAGA-3', antisense primer 5'-GGAGTGCAGGGTCCGAGGT-3') synthesized by Beijing SBS Genetech Co., Ltd., Beijing, China. Glycerol-3-phosphate dehydrogenase (GAPDH) was used as the internal reference.

Western blot analysis

Whole-cell lysates were prepared using cell lysis buffer (Invitrogen) supplemented with a protease inhibitor cocktail and 1 mM phenylmethylsulfonyl fluoride (Thermo Fisher Scientific, Waltham, MA, USA). Protein concentrations were measured using a bicinchoninic acid (BCA) assay kit (Thermo Fisher Scientific), and then 30 μg of proteins were separated by polyacrylamide gel electrophoresis. After electrotransfer to polyvinylidene difluoride membranes, non-specific binding sites were blocked with 5% non-fat milk in Tris-buffered saline with Tween 20 (TBST) for 1 hour at room temperature. Membranes were incubated with anti-homeobox A7 (HOXA7) and anti-GAPDH primary antibodies (Abcam, Cambridge, MA, USA) overnight at 4°C, washed with TBST and then incubated with an anti-rabbit horseradish peroxidase-conjugated IgG secondary antibody (Abcam) for 1 hour at room temperature. Immune complexes were visualized using enhanced chemiluminescence. GAPDH was used as an internal control. The gray value of protein bands was analyzed by ImageJ software (National Institutes of Health, Bethesda, MD, USA).

Bioinformatics analysis

The circVAPA sequence was used as an input in the StarBase database (<http://starbase.sysu.edu.cn/>), which identifies more than 1.1 million miRNA-ncRNA interactions.

RNA pull-down assay

Cell lysates were collected with IP lysis buffer (Beyotime, Beijing, China) and incubated with biotinylated circVAPA and control oligos (Beijing SBS Genetech Co., Ltd.). Then, 10% of the lysates was saved as the input. The mixture was further incubated with M-280 streptavidin magnetic beads (Sigma-Aldrich) at 4°C with shaking overnight. A magnetic bar was used to pull down the magnetic beads and associated nucleic acids, and then the samples were washed four times with a high-salt wash buffer. Both the input and elutes from the pull-down were purified with Trizol reagent (Invitrogen) in accordance with the manufacturer's protocol. Reverse transcription was carried out using Superscript III transcriptase (Invitrogen), and RT-qPCR analysis was performed using Maxima SYBR Green/ROX qPCR Master Mix (Thermo Fisher Scientific) on a LightCycler® 96 real-time PCR system (Roche, Grenzacherstrasse, Basel, Switzerland).

Statistical analyses

All experiments were repeated three times. Data were expressed as the mean \pm standard deviation (SD). The relationship between circVAPA expression and the clinicopathological data of patients with oral cancer was analyzed by chi-square tests. Kaplan–Meier survival curve and long-rank analyses were used to evaluate the relationship between circVAPA expression and the overall survival (OS) and progression-free survival time (PFS) of patients. Statistical analysis was performed

using IBM SPSS Statistics for Windows, Version 19.0 (IBM Corp., Armonk, NY, USA). One-way analysis of variance or student's t test was performed to analyze the difference among/between groups. $P < 0.05$ was considered to indicate a statistically significant difference.

Results

CircVAPA was highly expressed in oral cancer tissues and cells

Oral cancer and paracancer tissue samples were collected from 60 patients who underwent surgical resection. The results of RT-qPCR showed that circVAPA expression was increased in both oral cancer tissues and cell lines ($P < 0.001$) (Figure 1a, 1b). According to the cut-off value of circVAPA expression in oral cancer tissues, patients with oral cancer were divided into a high circVAPA expression group ($n = 30$) and low circVAPA expression group ($n = 30$). Kaplan–Meier survival curves showed that the OS and PFS of patients with oral cancer and high circVAPA expression were significantly shorter than those with low expression ($P < 0.05$, Figure 1c, 1d). circVAPA expression was found to be closely related to tumor size, TNM stage and distant metastasis ($P < 0.05$) but not age, sex or tumor differentiation (Table 1).

circVAPA knockdown inhibited the proliferation, migration and invasion of oral cancer cells

The highest expression of circVAPA was detected in Cal-27 cells. Therefore, we selected Cal-27 cells for further loss-of-function studies. The RT-qPCR results showed that, compared with si-NC, si-circVAPA#1 and si-circVAPA#2 effectively knocked down the expression of circVAPA in Cal-27 cells with an efficiency greater than 50% ($P < 0.001$, Figure 2a).

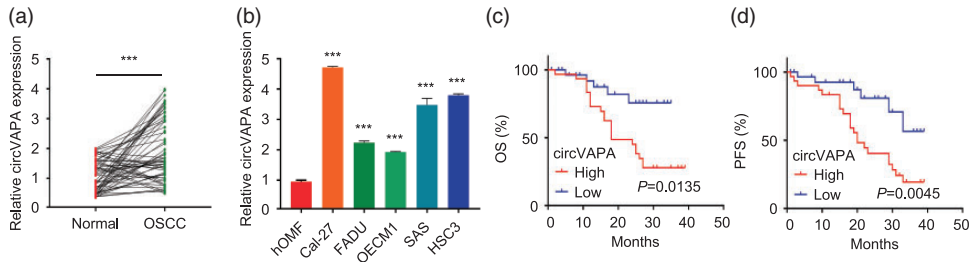


Figure 1. circVAPA is highly expressed in oral cancer tissues and cells. a: RT-qPCR was used to detect the expression level of circVAPA in 60 pairs of oral squamous cell carcinoma (OSCC) cancer tissues and corresponding adjacent normal tissues. $***P < 0.001$. b: RT-qPCR was used to detect the expression of circVAPA in oral cancer cell lines (Cal-27, FaDu, OECM1, SAS, HSC3) and human oral mucous fibroblasts (hOMFs). $***P < 0.001$ compared with hOMFs. c: Kaplan–Meier survival curve analysis was used to evaluate the overall survival (OS) of patients with oral cancer who showed low circVAPA expression ($n = 30$) and high circVAPA expression ($n = 30$). The survival curves were compared with the log-rank test. d: Kaplan–Meier survival curve analysis was used to evaluate the progression-free survival (PFS) of patients with oral cancer who showed low circVAPA expression ($n = 30$) and high circVAPA expression ($n = 30$). The survival curves were compared with the log-rank test

Table 1. Correlations of circVAPA expression with clinicopathologic features of patients with oral cancer

Factor	circVAPA expression		P-value
	Low (n=30)	High (n=30)	
Age			0.197
≤60 years	17	12	
>60 years	13	18	
Sex			0.606
Men	15	18	
Women	15	12	
Tumor size			0.010
≤2 cm	19	9	
>2 cm	11	21	
Tumor differentiation			0.302
I	17	13	
II	13	17	
T classification			0.0389
T1–T2	18	11	
T3–T4	11	19	
N classification			0.020
N0–N1	20	11	
N2–N3	10	19	
Clinical stage			0.002
I/II	18	6	
III/IV	12	24	
Distant metastasis			<0.001
Yes	9	25	
No	21	5	

Chi-square test was used to analyze the relationship between circVAPA expression and clinicopathological data.

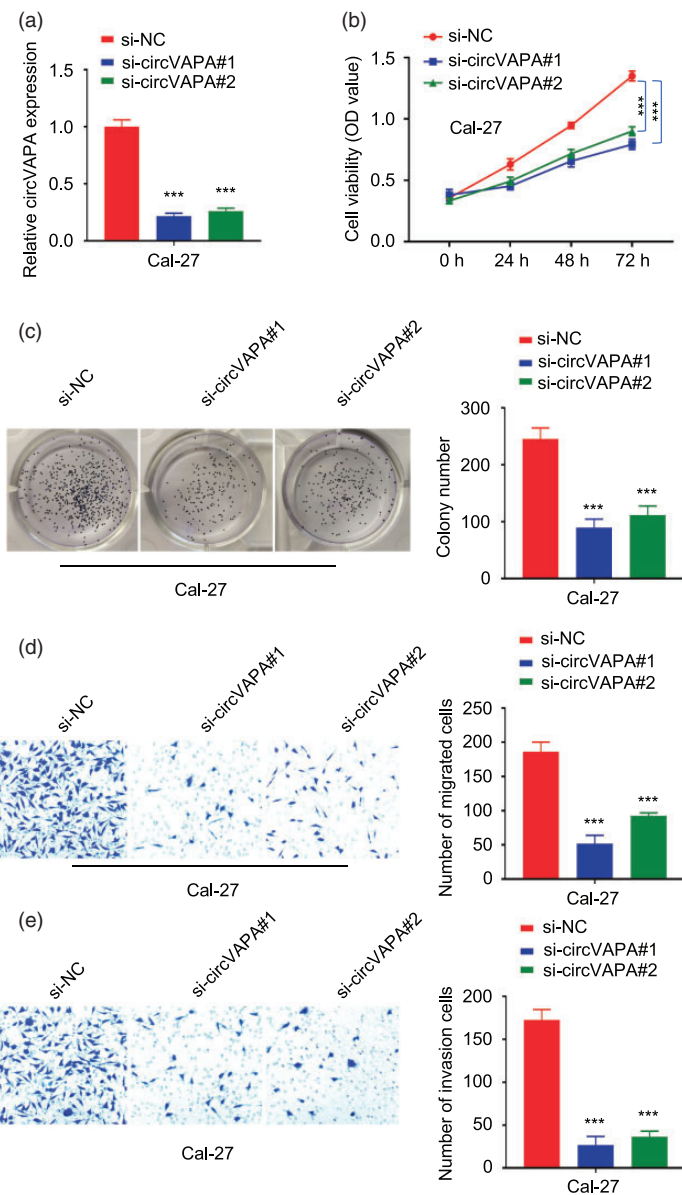


Figure 2. CircVAPA knockdown inhibits the proliferation, migration and invasion of oral cancer cells. a: Two siRNA targeting circVAPA (si-circVAPA#1 and si-circVAPA#2) were designed to knock down circVAPA expression. A negative control (NC) siRNA was also used. The Cal-27 cell line with the highest expression of circVAPA was selected for silencing experiments. The knockdown efficiency was detected by RT-qPCR. *** $P < 0.001$ compared with si-NC. b: The cell counting kit-8 method was used to detect the optical density (OD) values of Cal-27 cells in different groups (si-NC, si-circVAPA#1, si-circVAPA#2) at 450 nm at 0, 24, 48 and 72 hours. *** $P < 0.001$. c: The clone formation ability of Cal-27 cells in different groups was detected and quantified. *** $P < 0.001$ compared with si-NC. d: Transwell assay (without Matrigel) was used to detect the migration ability of Cal-27 cells in different groups. *** $P < 0.001$ compared with si-NC. e: Transwell assay (with Matrigel) was used to detect the invasion ability of Cal-27 cells in different groups. *** $P < 0.001$ compared with si-NC

The CCK-8 results showed that circVAPA knockdown significantly reduced the cell viability of Cal-27 cells ($P < 0.01$, Figure 2b). The results of clone formation experiments showed that knockdown of circVAPA expression significantly reduced the colony formation ability of Cal-27 ($P < 0.01$, Figure 2c). The results of Transwell experiments showed that knockdown of circVAPA expression significantly reduced the migratory (without Matrigel, Figure 2d) and invasive (with Matrigel, Figure 2e) abilities of oral cancer cells (both $P < 0.01$).

CircVAPA targets miR-132

Through the analysis of the online StarBase database, a miR-132 binding site was identified in circVAPA. Luciferase reporter assay results showed that compared with miR-NC, miR-132 overexpression inhibited the luciferase activity of the wild-type circVAPA vector in Cal-27 cells. Mutation of the predicted miR-132 binding site abolished its inhibitory effect ($P < 0.001$) (Figure 3a). The results of RNA pull-down tests with a biotin-labeled circVAPA probe showed that compared with the oligo probe, the circVAPA probe pulled down significantly more miR-132 ($P < 0.01$, Figure 3b). qRT-PCR results showed that compared with si-NC, the expression of miR-132 was upregulated after the knockdown of circVAPA expression ($P < 0.01$), as shown in Figure 3c.

Inhibition of miR-132 partially reverses the effect of circVAPA knockdown in oral cancer cells

RT-qPCR showed that transfection with miR-132 inhibitor significantly decreased the expression of miR-132 ($P < 0.01$), as shown in Figure 4a. The CCK-8 results showed that knockdown of circVAPA expression significantly reduced the cell viability of Cal-27 cells, and when miR-132

inhibitor was cotransfected, the viability was partially increased ($P < 0.01$, Figure 4b). The results of clone formation experiments showed that circVAPA knockdown reduced the colony forming ability of Cal-27 cells, which was partially restored in cells cotransfected with miR-132 inhibitor ($P < 0.01$, Figure 4c). Transwell analyses (without Matrigel) showed that circVAPA knockdown reduced the migratory ability of Cal-27 cells, which was partially restored in cells cotransfected with miR-132 inhibitor ($P < 0.01$, Figure 4d). Similarly, knockdown of circVAPA expression reduced the invasion ability (with Matrigel) of Cal-27 cells, which was partially restored in the presence of miR-132 inhibitor ($P < 0.01$, Figure 4e).

circVAPA regulated HOXA7 protein expression by targeting miR-132

According to the prediction of the miR-132 binding site in the 3'-untranslated region (UTR) of HOXA7 by StarBase, luciferase reporter experiments were performed in Cal-27 cells. The results showed that compared with miR-NC, miR-132 overexpression inhibited the luciferase activity in these cells. After the predicted HOXA7 3'-UTR binding site was mutated, its inhibitory effect was abolished, as shown in Figure 5a ($P < 0.001$). Western blot results revealed a decreased protein expression level of HOXA7 in miR-132-overexpressing Cal-27 cells ($P < 0.001$) (Figure 5b). Additionally, circVAPA knockdown reduced the cellular expression level of HOXA7. When miR-132 inhibitor was cotransfected, the protein expression level of HOXA7 was partially increased ($P < 0.01$) (Figure 5c).

Discussion

Early diagnosis is important for the treatment and prognosis of oral cancer.¹⁵⁻¹⁷

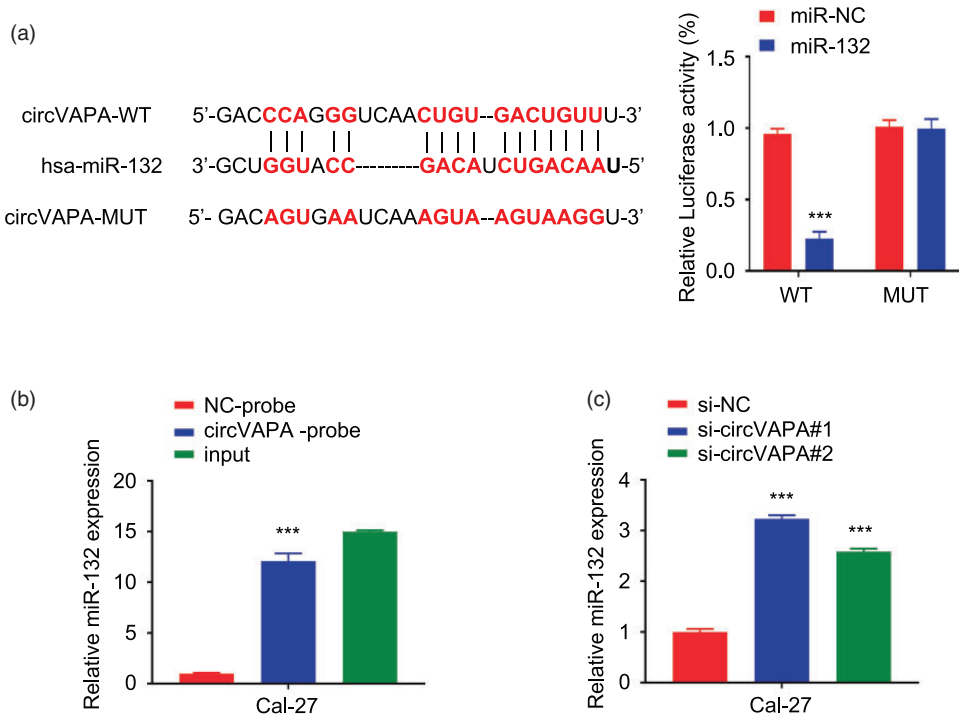


Figure 3. CircVAPA targets miR-132. a: The online StarBase database predicted a miR-132 binding site in the 3'-untranslated region (UTR) of wildtype (WT) circVAPA. This site was then mutated (MUT). Luciferase reporter experiments were carried out in Cal-27 cells transfected with a negative control (NC) or miR-132. *** $P < 0.001$ compared with miR-NC. b: The RNA pull-down assay with a biotin-labeled circVAPA probe confirmed that circVAPA directly interacted with miR-132. Input=10% of total lysate. *** $P < 0.001$ compared with NC-probe. c: RT-qPCR was used to detect the expression of miR-132 in Cal-27 cells. *** $P < 0.001$ compared with si-NC

Traditionally, invasion and metastasis are late events in the progression of oral cancer.^{17–19} At present, it is believed that during the early stage of oral cancer, tumor cells have begun to infiltrate,^{20,21} but the regulatory mechanism unclear.

Studies have shown that circ RNA plays an important role in the occurrence and development of a variety of malignant tumors.^{22–25} For example, circVAPA is highly expressed in colon cancer,²⁶ breast cancer²⁷ and liver cancer.²⁸ As an oncogene, circVAPA promotes the progression of tumor cells. The overexpression of circVAPA in breast cancer cells enhances

proliferation, invasion and migration. Conversely, its downregulated expression impairs the malignant behavior of breast cancer cells.²⁶ In colon cancer, the expression level of circVAPA is significantly increased, leading to increased proliferation and invasion.²⁶ The results of the current study showed that circVAPA was highly expressed in oral cancer tissues and cells, and its expression level was closely related to tumor size, TNM stage and distant metastasis. The OS and PFS of patients with oral cancer who showed high circVAPA expression were significantly shorter than those of patients with low

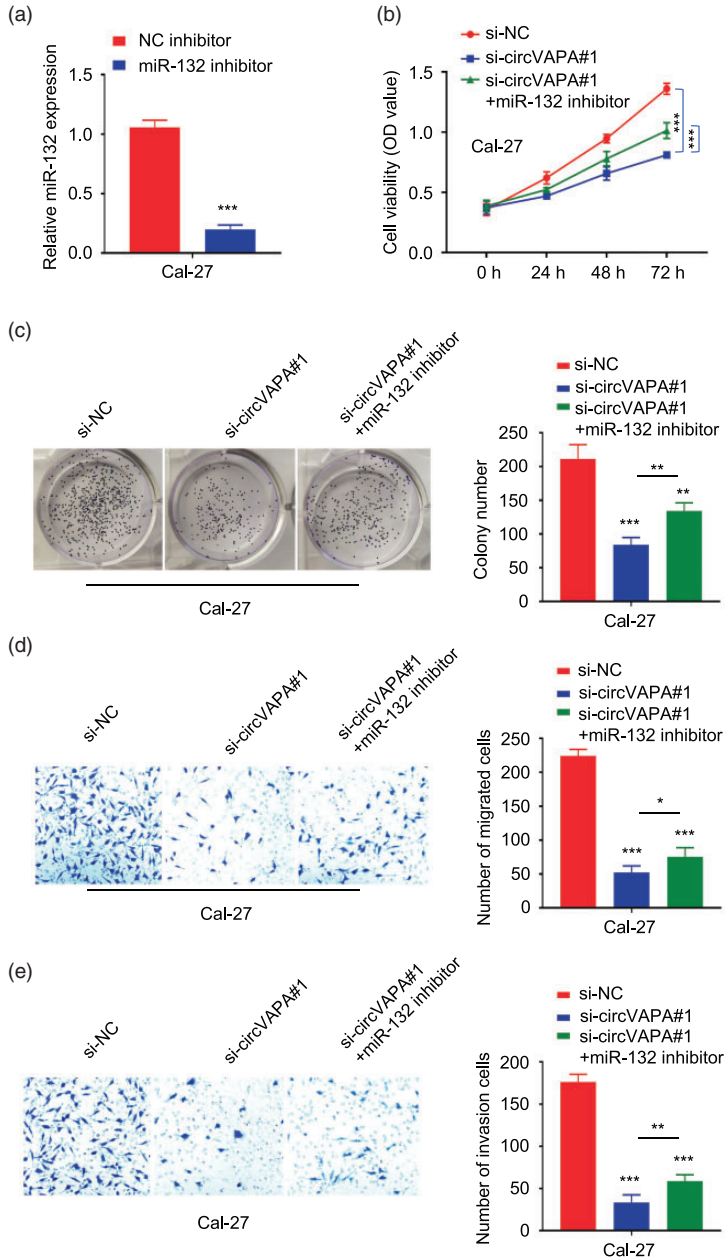


Figure 4. Inhibition of miR-132 partially reverses the effect of circVAPA knockdown in oral cancer cells. a: RT-qPCR was used to detect the expression of miR-132 in cells transfected with a negative control (NC) or miR-132 inhibitor. *** $P < 0.001$ compared with NC inhibitor. b: The cell counting kit-8 method was used to detect the cell viability at 0, 24, 48 and 72 hours in different groups indicated by the optical density (OD). *** $P < 0.001$. c: The clone formation ability of Cal-27 cells in different groups was detected by clone formation assays. ** $P < 0.01$ and *** $P < 0.001$. d: Transwell assay (without Matrigel) was used to detect the migration ability of Cal-27 cells in different groups. * $P < 0.05$, *** $P < 0.001$. e: Transwell assay (with Matrigel) was used to detect the invasion ability of Cal-27 cells in different groups. ** $P < 0.01$ and *** $P < 0.001$

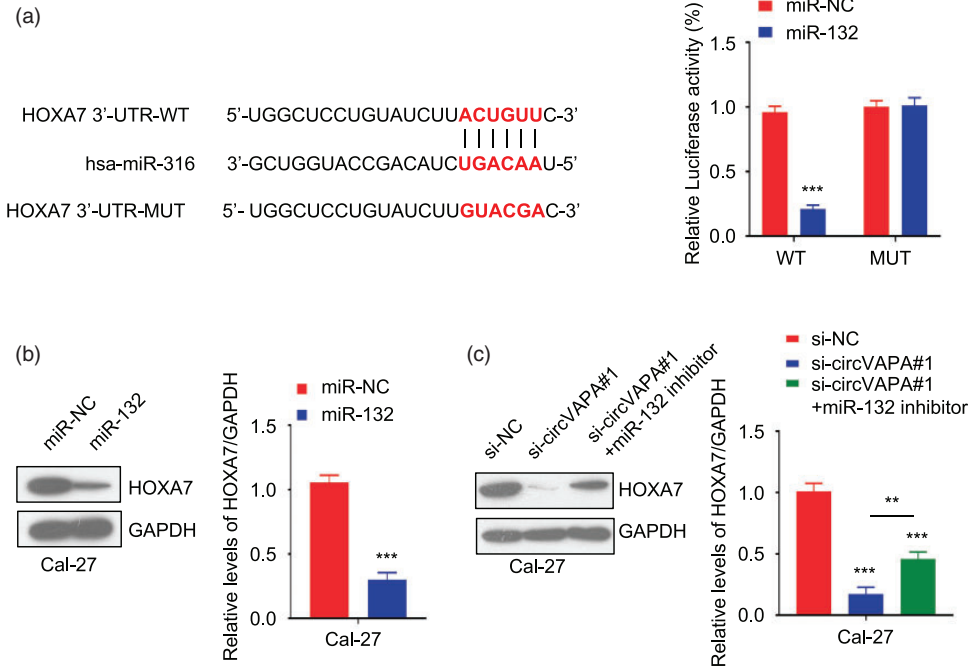


Figure 5. circVAPA regulates homeobox A7 (HOXA7) protein expression by targeting miR-132. a: The online StarBase database predicted a miR-132 binding site in the 3'-untranslated region (UTR) of wildtype (WT) circVAPA. This site was then mutated (MUT). Luciferase reporter experiments were carried out in Cal-27 cells transfected with a negative control (miR-NC) or miR-132. *** $P < 0.001$ compared with miR-NC. b: The protein expression of HOXA7 in Cal-27 cells overexpressing miR-132 was detected by western blot. *** $P < 0.001$ compared with miR-NC. Glycerol 3-phosphate dehydrogenase (GAPDH) was used as an internal control. c: HOXA7 protein expression level in different groups of Cal-27 cells was detected by western blot. ** $P < 0.01$ and *** $P < 0.001$. GAPDH was used as an internal control

expression of circVAPA, indicating that circVAPA is related to the prognosis of these patients. In addition, we found that knockdown of circVAPA expression in oral cancer cells inhibited their proliferation, migration and invasion. These results suggest that circVAPA may play a carcinogenic role in oral cancer. Therefore, inhibiting the expression of circVAPA may prevent the malignant progression of oral cancer.

Circ RNA is highly expressed and stable in cells. It can rapidly bind to or release a large number of miRNAs from their downstream target genes to effectively regulate miRNAs.²⁹⁻³¹ In glioblastoma, ciRS-7

adsorbs miR-7 and significantly inhibits its activity, leading to the upregulated expression of miR-7 target genes and increased tumor malignancy.³² In this study, the binding site of miR-132 in circVAPA was predicted by bioinformatics analysis and dual luciferase reporter assays. After knockdown of circVAPA, the expression of miR-132 was upregulated, indicating that miR-132 is a downstream target of circVAPA and that circVAPA negatively regulates miR-132. In addition, this study confirmed that there was a miR-132 binding site in the 3'-UTR of HOXA7. Overexpression of miR-132 decreased the protein expression of HOXA7, indicating that HOXA7 is a

downstream target of miR-132 and that miR-132 negatively regulates HOXA7. In addition, inhibition of miR-132 partially reversed the effects of circVAPA knock-down on the proliferation, invasion and migration of oral cancer cells. When cells were cotransfected with miR-132 inhibitor, the protein expression level of HOXA7 was partially increased, which indicated that circVAPA regulated the occurrence and progression of oral cancer through the miR-132/HOXA7 signaling axis.

In conclusion, circVAPA is upregulated in oral cancer, and its abnormal expression is related to the prognosis of patients with oral cancer. Inhibition of circVAPA expression inhibits the proliferation, migration and invasion of oral cancer cells, and its mechanism is related to the targeted regulation of the miR-132/HOXA7 signaling axis.

Declaration of conflicting interest

The authors declare that there is no conflict of interest.

Funding

This research received no specific grant from any funding agency in the public, commercial, or not-for-profit sectors.

ORCID iDs

Hao Chen  <https://orcid.org/0000-0003-1495-0739>

Xiaoyong Qiu  <https://orcid.org/0000-0003-0848-3636>

References

1. Bao X, Liu F, Chen Q, et al. Propensity score analysis exploring the impact of smoking and drinking on the prognosis of patients with oral cancer. *Head Neck* 2020; 42: 1837–1847.
2. Sliker FJB, De Bree R and Van Cann EM. Oral squamous cell carcinoma involving the maxillae: Factors affecting local recurrence and the value of salvage treatment for overall survival. *Head Neck* 2020; 42: 1821–1828.
3. Mermod M, Jourdan EF, Gupta R, et al. Development and validation of a multivariable prediction model for the identification of occult lymph node metastasis in oral squamous cell carcinoma. *Head Neck* 2020; 42: 1811–1820.
4. Retraction: MUC1 gene silencing inhibits proliferation, invasion and migration while promoting apoptosis of oral squamous cell carcinoma cells. *Biosci Rep* 2020; 40: BSR-20182193_RET.
5. Si X, Zheng H, Wei G, et al. circRNA Hipk3 Induces Cardiac Regeneration after Myocardial Infarction in Mice by Binding to Notch1 and miR-133a. *Mol Ther Nucleic Acids* 2020; 21: 636–655.
6. Yan Y, Yang J, Pathak JL, et al. CircRNA_104889 promotes lung adenocarcinoma cell invasion via sponging miR4458. *Cancer Cell Int* 2020; 20: 1–12.
7. Chen ZG, Zhao HJ, Lin L, et al. Circular RNA CirCHIPK3 promotes cell proliferation and invasion of breast cancer by sponging miR - 193a/HMGB1/PI3K/AKT axis. *Thorac Cancer* 2020; 11: 2660–2671.
8. Zhang W, Shi J, Cheng C, et al. CircTIMELESS regulates the proliferation and invasion of lung squamous cell carcinoma cells via the miR-136-5p/ROCK1 axis. *J Cell Physiol* 2020; 235: 5962–5971.
9. Yao QP, Liu Z, Yao AH, et al. Circular RNA circTET3 mediates migration of rat vascular smooth muscle cells by targeting miR-351-5p. *J Cell Physiol* 2020; 235: 6831–6842.
10. Chen C, Yin P, Hu S, et al. Circular RNA-9119 protects IL-1 β -treated chondrocytes from apoptosis in an osteoarthritis cell model by intercepting the microRNA-26a/PTEN axis. *Life Sci* 2020; 256: 117924.
11. Yang S, Jiang Y, Ren X, et al. FOXA1-induced circOSBPL10 potentiates cervical cancer cell proliferation and migration through miR-1179/UBE2Q1 axis. *Cancer Cell Int* 2020; 20: 389.
12. Fan HY, Jiang J, Tang YJ, et al. CircRNAs: A New Chapter in Oral Squamous Cell Carcinoma Biology. *Onco Targets Ther* 2020; 13: 9071–9083.

13. Zhang X, Xu Y, Yamaguchi K, et al. Circular RNA circVAPA knockdown suppresses colorectal cancer cell growth process by regulating miR-125a/CREB5 axis. *Cancer Cell Int* 2020; 20: 103.
14. Amin MB, Edge S, Greene F, et al. *AJCC Cancer Staging Manual*. 8th ed New York: Springer, 2017.
15. Mroueh R, Nevala A, Haapaniemi A, et al. Risk of second primary cancer in oral squamous cell carcinoma. *Head Neck* 2020; 42: 1848–1858.
16. Malik A, Nair S, Singh A, et al. Soft tissue deposit in neck dissection specimen carries a poor prognosis in oral cancer: A matched pair analysis. *Head Neck* 2020; 42: 1783–1790.
17. Alshehri BM. Trends in the incidence of oral cancer in Saudi Arabia from 1994 to 2015. *World J Surg Oncol* 2020; 18: 217.
18. Do Carmo AF, Dourado MR, De Oliveira CE, et al. Stanniocalcin 2 contributes to aggressiveness and is a prognostic marker for oral squamous cell carcinoma. *Exp Cell Res* 2020; 393: 112092.
19. Goetz C, Raschka J, Wolff KD, et al. Hospital Based Quality of Life in Oral Cancer Surgery. *Cancers (Basel)* 2020; 12: 2152.
20. Yamagata K, Fukuzawa S, Ishibashi-Kanno N, et al. The Association between D-Dimer and Prognosis in the Patients with Oral Cancer. *Dent J (Basel)* 2020; 8: 84.
21. Dalmartello M, Decarli A, Ferraroni M, et al. Dietary patterns and oral and pharyngeal cancer using latent class analysis. *Int J Cancer* 2020; 147: 719–727.
22. Kong R. Circular RNA hsa_circ_0085131 is involved in cisplatin-resistance of non-small-cell lung cancer cells by regulating autophagy. *Cell Biol Int* 2020; 44: 1945–1956.
23. Lu C, Fu L, Qian X, et al. Knockdown of circular RNA circ-FARSA restricts colorectal cancer cell growth through regulation of miR-330-5p/LASP1 axis. *Arch Biochem Biophys* 2020; 689: 108434.
24. Hui C, Tian L and He X. Circular RNA circNHSL1 Contributes to Gastric Cancer Progression Through the miR-149-5p/YWHAZ Axis. *Cancer Manag Res* 2020; 12: 7117–7130.
25. Liu H, Bi J, Dong W, et al. Correction to: Invasion-related circular RNA circFNDC3B inhibits bladder cancer progression through the miR-1178-3p/G3BP2/SRC/FAK axis. *Mol Cancer* 2020; 19: 124.
26. Li XN, Wang ZJ, Ye CX, et al. Circular RNA circVAPA is up-regulated and exerts oncogenic properties by sponging miR-101 in colorectal cancer. *Biomed Pharmacother* 2019; 112: 108611.
27. Zhou SY, Chen W, Yang SJ, et al. Circular RNA circVAPA regulates breast cancer cell migration and invasion via sponging miR-130a-5p. *Epigenomics* 2020; 12: 303–317.
28. Liu C, Zhong X, Li J, et al. Circular RNA circVAPA Promotes Cell Proliferation in Hepatocellular Carcinoma. *Hum Gene Ther Clin Dev* 2019; 30: 152–159.
29. Zhang F, Xu Y, Ye W, et al. Circular RNA S-7 promotes ovarian cancer EMT via sponging miR-641 to up-regulate ZEB1 and MDM2. *Biosci Rep* 2020; 40: BSR20200825.
30. Zhang PR, Ren J, Wan JS, et al. Circular RNA hsa_circ_0002052 promotes osteosarcoma via modulating miR-382/STX6 axis. *Hum Cell* 2020; 33: 810–818.
31. Hao Y, Xi J, Peng Y, et al. Circular RNA Circ_0016760 Modulates Non-Small-Cell Lung Cancer Growth Through the miR-577/ZBTB7A Axis. *Cancer Manag Res* 2020; 12: 5561–5574.
32. Liu L, Liu FB, Huang M, et al. Circular RNA ciRS-7 promotes the proliferation and metastasis of pancreatic cancer by regulating miR-7-mediated EGFR/STAT3 signaling pathway. *Hepatobiliary Pancreat Dis Int* 2019; 18: 580–586.